View of Normal Human Skin *In Vivo* as Observed Using Fluorescent Fiber-Optic Confocal Microscopic Imaging

Lucinda D. Swindle,*†‡ Steven G. Thomas,‡ Michael Freeman,*§ and Peter M. Delaney‡

*The Skin Center, Suite 5, Queensland, Australia; §The Gold Coast Hospital, Queensland, Australia; ‡Optiscan, Victoria, Australia; †Dermatology Service, Memorial Sloan-Kettering Cancer Center, New York, New York, USA

Fluorescence confocal scanning laser microscopy, using a miniaturized handheld scanner, was performed to visualize the microscopic architecture of normal human epidermis *in vivo*. Fluorescein sodium (~20 μL of 0.2% wt/vol) was administered via intradermal injection to normal skin on the volar forearm of 22 patients. The skin was imaged continuously from 1 to 15 min after injection. Fluorescein was excited at 488 nm and the fluorescent emission was detected at >505 nm. In each subject, a series of images was collected at increasing depth, from superficial stratum corneum to papillary dermis. Features observed in confocal images were compared to those seen in hematoxylin- and eosin-stained sections of skin. The confocal images demonstrated the architecture of superficial skin in the horizontal plane. There was a transition in keratinocyte size, shape, and morphology with progressive imaging into the deeper epidermal layers. Superficial dermis and microscopic capillaries with blood flow were easily observed. The morphologic patterns associated with the major cell types of the epidermis were consistent with those known from conventional histology. We report the ability of *in vivo* fluorescence point scanning laser confocal microscopy to produce real-time, high-resolution images of the microscopic architecture of normal human epidermis using a noninvasive imaging technology. *J Invest Dermatol 121:706–712, 2003*

Confocal scanning laser microscopy (CSLM) allows visualization of subsurface detail in living human skin by means of its ability to perform optical sectioning (New *et al*, 1991). The technology optically rejects out of focus light and only detects light from the focal plane. The focal plane is positioned below the tissue surface to enable subsurface imaging. The confocal technique enables preservation of the tissue's physical structure whilst being studied in its physiologic state *in vivo* and can also observe dynamic processes both in real time (Papworth *et al*, 1998) and by sequential imaging of the same site (Gonzalez *et al*, 1999a; Aghassi *et al*, 2000b). In contrast, light microscopy of biopsy specimens requires an extensive preparative protocol (fixation, sectioning, mounting, and staining), giving rise to the potential for artifacts (Bloom and Fawcett, 1975) and disruption of the cell's native structure and environment. Furthermore, histologic sections from a biopsy only demonstrate tissue morphology at one point in time.

Fiber-optic elements may be used in various ways to miniaturize or bring flexibility to the implementation of confocal microscopes (Gmitro and Aziz, 1993; Delaney and Harris, 1995; Juskaitis *et al*, 1997; Liang *et al*, 2002). This study utilized an implementation that uses one single-moded optical fiber acting as a spatial filter (pinhole) in both the illumination and the detection light paths. This results in optical sectioning performance comparable to bulk optical implementations of point scanning confocal microscopes (Delaney and Harris, 1995; Delaney *et al*, 1994a). This fiber-optic approach has enabled miniaturization of the scanner and objective optics of the confocal microscope into a handheld device that provides flexibility and mobility, thus being convenient for *in vivo* and clinical use.

Imaging of human epidermis and superficial dermis *in vivo* has been demonstrated using reflectance confocal microscopy (Rajadhyaksha *et al*, 1999; Corcuff *et al*, 2001). Such use of reflectance confocal imaging has exploited inherent differences in the reflectivity (or refractive index) of microstructures within and between cells to produce contrast, at specific illumination wavelengths. For example, in these studies, strong image contrast is associated with distribution of naturally occurring components of tissue such as melanin or keratin, which have been shown to strongly backscatter at near-infrared wavelengths (Rajadhyaksha *et al*, 1995). Several studies have established the relationship between reflectance confocal images and known pathologies (Gonzalez *et al*, 1999a, b, c; Aghassi *et al*, 2000a; Busam *et al*, 2001a, b; Langley *et al*, 2001; Rajadhyaksha *et al*, 2001; Charles *et al*, 2002; Gonzalez and Tannous, 2002; Sauermann *et al*, 2002).

There are limited reports of *in vivo* fluorescence confocal microscopy utilizing exogenous fluorophores in human skin to date (Swindle *et al*, 2002; Thorn Leeson *et al*, 2002). CSLM in fluorescence mode relies on the differential distribution of endogenous or exogenous fluorescent molecules (fluorophores) to produce contrast (Delaney *et al*, 1993). A laser light source, at an appropriate wavelength, is used to excite the fluorophore, and the emitted fluorescence signal is detected simultaneously.

Manuscript received October 11, 2002; revised March 10, 2003; accepted for publication April 28, 2003

Reprint requests to: Peter Delaney, Optiscan, PO Box 1066, Mt Waverley MDC, Victoria, Australia, 3149. E-mail: peterd@optiscan.com

This work was performed at The Skin Center under ethics approval from the Gold Coast Hospital. Nevertheless, the manuscript and images were prepared when the first author's current affiliation was Memorial Sloan Kettering Cancer Center.

Abbreviation: CSLM, confocal scanning laser microscopy.

0022-202X/03/$15.00 · Copyright © 2003 by The Society for Investigative Dermatology, Inc.

Fluorescence confocal microscopy has been used to visualize selectively stained structures in the skin *ex vivo* and *in vitro*. Veiro and Cummins (1994) highlighted the potential for imaging targeted skin structures at the subcellular level, such as nuclei or lipids, with the use of an exogenous contrast agent. The fluorescent agents used, however, were not suitable candidates for *in vivo* studies.

In vivo fluorescence confocal microscopy studies using animal models have demonstrated a range of potential clinical applications for *in vivo* fluorescence CSLM. These have included characterization of epidermal layers and subcellular structure of skin (Bussau *et al*, 1998), mucous crypt architecture and subcellular detail of colon (Delaney *et al*, 1994b), blood flow in superficial vasculature of the skin (Delaney *et al*, 1993; Papworth *et al*, 1998), changes in microvasculature in skin pathologies (Vo *et al*, 2000; Anikijenko *et al*, 2001), and imaging of human melanoma using specific labeled antibodies (Anikijenko *et al*, 2001). To date, however, these potential applications have not been tested in humans. This study examines the potential of fluorescence CSLM, using a miniaturized handheld scanner in combination with an exogenous fluorescent contrast agent, to provide high-resolution images of human skin *in vivo*.

MATERIALS AND METHODS

Subjects Twenty-two patients (17 men and 5 women) ranging from 26 to 83 years of age comprised the study sample. Ethics approval was granted from the Gold Coast Hospital Ethics Committee and informed written consent was obtained from each patient. All patients were Caucasian, with skin types ranging from I to IV. Patients recruited were those attending the Dermatology Clinic for routine skin examination or excision of sun-related atypical lesions at other skin sites. Clinically normal, non-sun-damaged skin on the inner forearm was imaged with the confocal microscope.

***In vivo* fluorescence confocal microscopy** The imaging site on the volar surface of the forearm was prepared with a standard alcoholic preparation (AlcoWIPE, Erie Scientific, Portsmouth, NH) before the introduction of contrast agent. Approximately 20 μL of a 0.2% solution of fluorescein sodium was injected intradermally using a 30-gauge hypodermic needle. One drop of the same 0.2% fluorescein sodium solution was also applied topically to the same site to ensure adequate labeling of the stratum corneum. A drop of immersion oil (Olympus) was applied to the imaging site to reduce surface scattering effects.

Imaging was performed continuously from 1 to 15 min after introduction of the fluorescent contrast agent. This time frame was chosen after observations in a pilot study showed variation in the distribution of contrast agent within the viable cell layers after 20 min. In the pilot study it was observed that the fluorescein was initially confined to the extracellular spaces (bright cell borders and darker cytoplasm) and by approximately 20 min had redistributed considerably in some areas (bright cytoplasm and darker intercellular spaces). Beyond 30 min, image quality had deteriorated significantly with loss of consistent contrast between cellular structures. Therefore, the optimal time for this study to demonstrate consistent images was considered to be from injection time to 15 min later.

The imaging system comprised a modified confocal microscope (F900e personal confocal microscope system, Optiscan Pty Ltd, Australia) fitted with a novel miniaturized, vibrating fiber, handheld scanner (Delaney and Harris, 1995). The scanner was placed against the skin with gentle pressure to stabilize the tissue relative to the scanner optics. The cohesive movement of the scanner head with the subject minimized movement artifact in the image.

The tissue was illuminated with blue laser light (488 nm, <0.5 mW at the skin) with detection above 505 nm to capture the green fluorescent signal. The scanner included a customized objective lens system with an effective numerical aperture of approximately 0.5 and a scanned field of view of 250×250 μm. Images of 512×512 pixels were captured from this field of view and displayed at two frames per second. In pilot work, these parameters and the above-described protocol for fluorescein administration were found to result in strong fluorescent signal. At the instrument settings used to image the bright fluorescein signal, autofluorescence was undetectable.

Representative images at each layer of the epidermis were captured by varying the imaging depth, which was controlled by a lever on the scanner. Single scans of the tissue were captured, each representing one focal plane within the tissue. There was no processing of the images with software before analysis and reproduction for this paper.

Histology Histologic correlation was not sought from each individual patient because this was clinically normal skin being imaged and therefore biopsy was not indicated. One representative sample of normal skin was obtained from the normal margins of an excision of a pigmented lesion on the ventral forearm. This normal skin was fixed, sectioned vertically, and stained with hematoxylin and eosin as per conventional histologic technique. This allowed comparison of gross morphology in the confocal images to the more common histologic view of skin. Because the confocal images are an *en face* view, we also cut and stained sections of this normal skin in the horizontal plane to view with the conventional light microscope. This was helpful in the interpretation of the view offered by the confocal images.

RESULTS

***In vivo* fluorescence confocal microscopy demonstrates the microscopic architecture of normal human skin** The image sets taken for all 22 patients showed a clearly recognizable epidermal architecture, with images taken from the stratum corneum to the basal layer (**Fig 1**). The papillary dermis was viewed in all patients. Owing to the fact that the skin surface and the underlying layers of the epidermis undulate, whereas the focal plane of the confocal microscope is flat, most images feature focal regions of cells from different layers (**Figs 2, 3**). The named layers of the epidermis were identified in the confocal images by the morphologic characteristics of cells in each layer (which are well known from histology), together with their location relative to nearby distinctive structures (such as dermal papillae) and visual similarity to corresponding histology sections. Image quality improved over time, peaking between 3 and 5 min after introduction of the contrast agent.

Skin surface structures are clearly labeled with topical fluorescein The results (**Fig 1*a–j***) show confocal images at the same site at progressive depths from stratum corneum to papillary dermis. The superficial corneocytes (**Figs 1*a***, **4**) fluoresced avidly immediately after application of the topical fluorescein. There was no temporal change in fluorescein distribution in this layer of nonviable cells. The images of superficial planes showed irregular islands of large (15–30 μm), polygonal, flattened, anucleated corneocytes that overlap at their edges. There was variation from a relatively neat, flat array of cells in the deeper stratum compactum (**Fig 4**) to disorganized, folded, sloughing debris in the superficial stratum dysjunctum (**Fig 1*a***). The residual nuclei or remnants of apoptotic nuclei were noted in the deeper layers of stratum corneum, as the junction of stratum corneum and granulosum was approached (**Fig 4**).

At the skin surface, a brightly labeled hair (**Fig 4**) could often be seen emerging from a hair follicle. At all depths, the hair follicles were seen as large black empty ring structures (**Fig 1*a*,*c*,*e*,*g*,*i***), where contrast agent had not penetrated. The black follicles could be traced down through the depth of the epidermis and were useful landmarks for orientation. Wrinkles and creases in the topography of the skin were seen as bright fluorescent crevices near the surface as a result of pooling of topically applied fluorescein (**Fig 5**).

Fluorescence confocal microscopy of the viable epidermis results in consistent, reproducible images As depth was increased into the viable epidermal layers, large keratinocytes (20–30 μm) were arranged in a flat, cohesive array (**Figs 1*c***, **5**). Initially, the fluorescein was confined predominantly to the extracellular spaces (**Fig 1*c***). At the end of the imaging time (15 min), when fluorescein had begun to appear to redistribute to an intracellular location, these cells demonstrated a distinct cytoplasm containing fine, bright staining granules and a dark, large nucleus (**Fig 5**). The granular pattern in the cytoplasm is

consistent with the increased number of cytoplasmic organelles (keratohyaline granules and membrane coating granules) observed in the stratum granulosum in conventional histology (**Fig 1*d***). It should be noted that in all subjects a very thin, acellular, darker layer was briefly visible as imaging depth was increased from the stratum corneum to granulosum (**Fig 3*a***). Therefore, a region was observed which excluded fluorescein, both from above (topical) and from beneath (injected), consistent with the barrier function expected for the upper epidermis.

Keratinocytes in the underlying layers were markedly smaller (10–25 μm) and arranged in a distinctive honeycomb-like pattern (**Fig 1*e***). Contiguous, morphologically similar cells characterized these layers, their size and location consistent with the stratum spinosum. In real-time imaging, as layers within stratum spinosum were imaged from superficial to deep, a decrease in cell size was appreciated (**Fig 1*g***). Of particular note in the deeper regions of viable epidermis was the frequent presence of as yet unidentified, strongly fluorescent, variable-sized spots (see **Fig 1*g*** and Discussion).

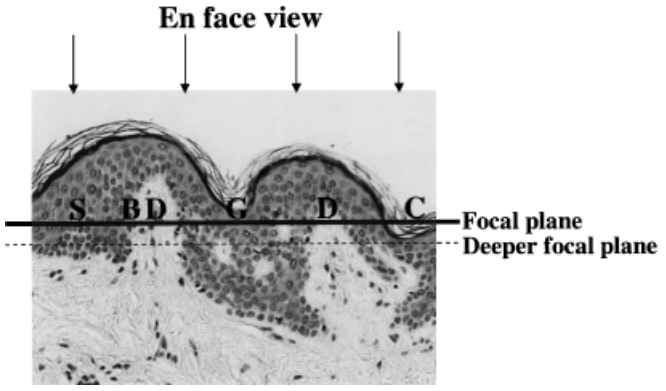

Figure 2. This vertical histology section illustrates the perpendicular view (*en face*) acquired by confocal imaging. Each planar confocal image (*thick black line*) may capture multiple different cell layers of the undulating epidermis. *S,* stratum spinosum; *B,* basal layer; *D,* dermis; *G,* stratum granulosum; *C,* stratum corneum. 20 × objective lens.

As imaging depth progressed toward the basal layer, the bright, homogeneous, acellular round "hilltops" of papillary dermis were observed interposed among the keratinocytes (**Figs 1*g*,*i***, **3*a***, **6*a***, **7*a***), as also demonstrated in comparative horizontal histologic sections (**Figs 1*h*,*j***, **3*b***, **6*b***, **7*b***). Small (7–12 μm), densely packed basal keratinocytes were circumferentially arranged around the papillae (**Figs 1*i***, **6**). As the dermal papillae were sectioned deeper with confocal slices, the images showed these round papillae increasing in size. Many of the individual basal cells surrounding the papillae were noted to have distinctly darker cytoplasm compared to cells in other layers (see **Fig 6*a*** and Discussion).

The approximate region of the dermoepidermal junction was predictable, with the presence of two factors, namely when the keratinocytes had reached minimal size and the bright

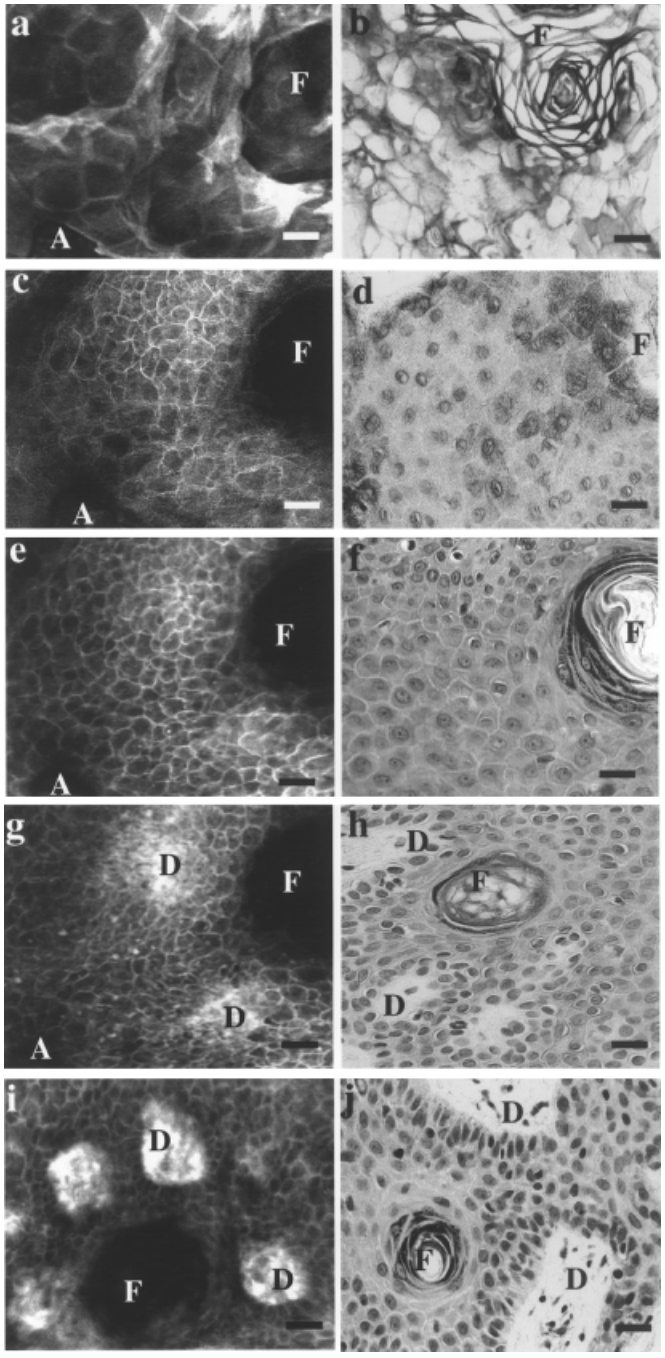

Figure 1. The microarchitecture of horizontal (*en face*) confocal sections (*a,c,e,g,i*) visually corresponds with horizontal hematoxylin- and eosin-stained histologic sections of epidermis and papillary dermis (*b,d,f,h,j*). The confocal images are captured at the same skin site, but at different depths below the skin surface. The distribution of the fluorescein is predominantly extracellular. A hair follicle (*F*) can be seen at all depths as a black ring structure. Artifact on the skin surface (oil bubbles and debris), and shadowing in the deeper layers from surface artifact (*A*) is distinguishable from normal skin structure. The changing morphology from stratum corneum to papillary dermis includes (*a,b*) large (15–30 μm) polygonal anucleated corneocytes. The bright areas are clumped and sloughing corneocytes. (*c,d*) Large (20–30 μm) rounded keratinocytes. The granular cytoplasm of cells at this layer is seen in the hematoxylin and eosin section (*d*). Correlating granular cytoplasm is seen in confocal images when the fluorescein has begun to redistribute to an intracellular location (see also **Fig 5**). (*e–h*) Honeycomb-like array of smaller (10–25 μm) keratinocytes in the spinous layer. A decrease in cell size was appreciated between upper (*e,f*) and lower (*g,h*) spinous layers. The dermal papillae hilltops (*D*) are seen in the lower spinous level (*g,h*). Strongly fluorescent, variable-sized spots in the confocal image (*bottom left of g*) have not been correlated with histology. (*i,j*) Small (7–12 μm) basal cells are arranged circumferentially around circular dermal papillae projections. The cytoplasm of basal cells is often darker than keratinocytes in upper layers, especially in subjects with darker skin (see also **Fig 6**). *Bar,* 25 μm.

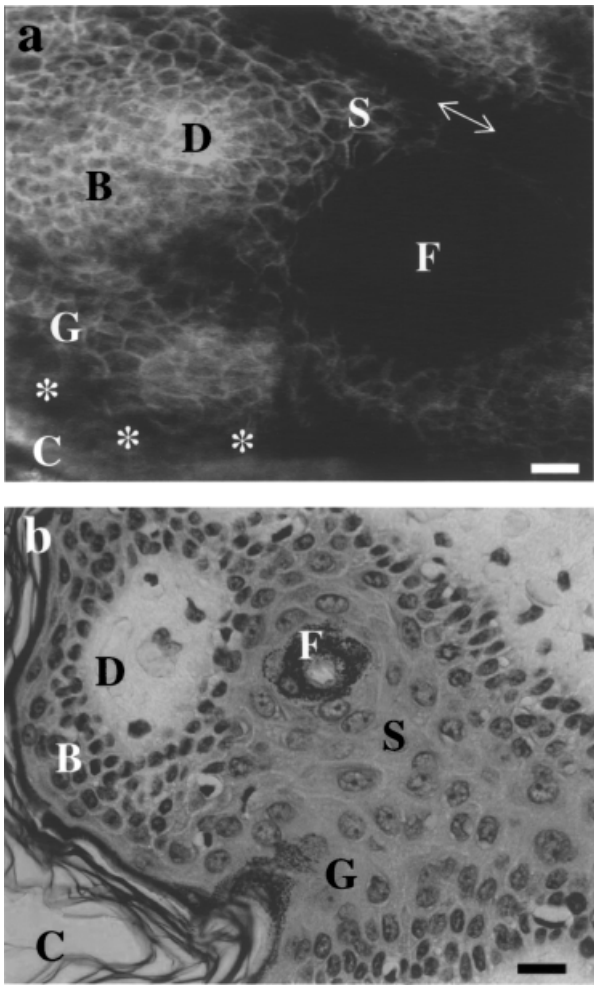

Figure 3. This *in vivo* confocal image (*a*) and horizontal histology section (*b*) show regions of cells from different layers. *C,* stratum corneum; *G,* stratum granulosum; *S,* stratum spinosum; *B,* basal layer; *D,* dermis; *F,* hair follicle. A bright hair at the surface has caused a shadow in the layers beneath (*a, double-headed white arrow*). When imaging from superficial to deep, a thin, acellular layer was passed through at the level of deep stratum corneum (***) where neither topical fluorescein from above nor intradermal fluorescein from below had labeled and therefore appearing darker. *Bar,* 25 μm.

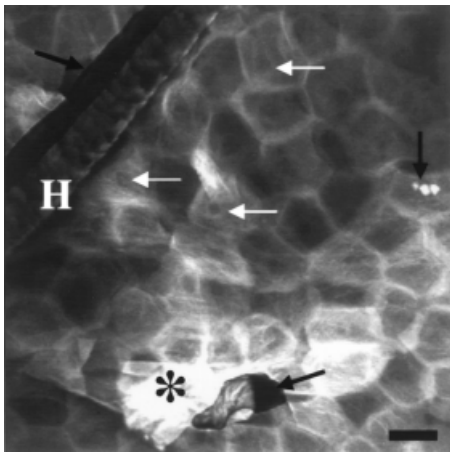

Figure 4. The surface topography showed clumps of sloughing corneocytes (*), fluorescein-labeled hairs emerging from follicles (*H*), and surface artifact (*black arrows,* oil bubbles next to hair; and *white spots,* debris). The slightly deeper cells in stratum compactum (*upper region*) have small central darker circles that are nuclear remnants (*white arrows*). *Bar,* 25 μm.

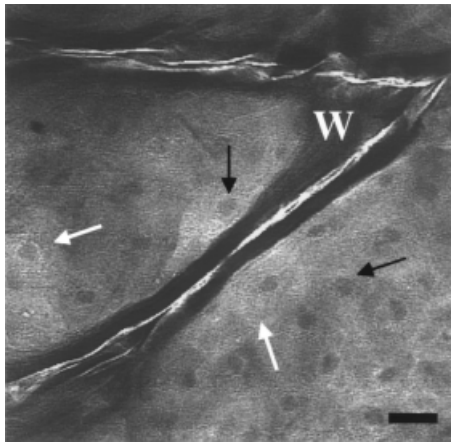

Figure 5. This confocal image shows keratinocytes at the junction of the deep stratum corneum and stratum granulosum. Some cells exhibit a granular cytoplasm (*white arrows*) and central dark nuclei (*black arrows*) when the fluorescein has begun to redistribute from an extracellular to an intracellular location. Wrinkles and creases (*W*) appear as bright lines where topical fluorescein has pooled. *Bar,* 25 μm.

homogeneous hilltops of the papillary dermis were in view. Capillary loops seen clearly in the dermal papillae (**Fig 7**) displayed the dynamic process of blood flow when imaging *in vivo.* Tumbling blood cells were visible as black disks contrasting with bright plasma in the capillary lumen (**Fig 7*a***). The plasma appeared to be a predominant form of clearance for the contrast agent, as the capillary structures became more fluorescent over time, whereas conversely, the contrast faded in the epidermal layers.

In skin of (certain) subjects with relatively thin epidermis, imaging into superficial reticular dermis was possible. As maximal depth of fluorescence was approached, by shifting the depth of the focal plane further into the tissue, the deepest of the basal keratinocytes were seen in the troughs of rete ridges and the individual dermal papillae coalesced into continuous bright sheets of reticular dermis.

Artifact in the confocal images is distinguishable from normal skin structure Sources of artifact in the confocal images included spherical aberration caused by oil bubbles at the surface (**Figs 1, 4**) and bright streaks or spots caused by debris sticking to the glass coverslip (**Fig 4**). These were quite distinct and recognizable structures and therefore not confused with normal skin structure. Bright structures at the surface with large amounts of fluorescent emission, such as hairs, clumps of sloughing corneocytes, and wrinkles, tended to cause shadowing in the layers directly beneath. (**Figs 1*c*,*e*,*g*, 3**)

DISCUSSION

In vivo confocal microscopy is being widely established as a useful investigative tool in the study of skin morphology and skin diseases. To date, the majority of reports of *in vivo* confocal microscopy of human skin have used reflectance mode. We report the feasibility of producing real-time, high-resolution images of intact living human skin, using a novel handheld fluorescence laser scanning confocal microscope in combination with an exogenous

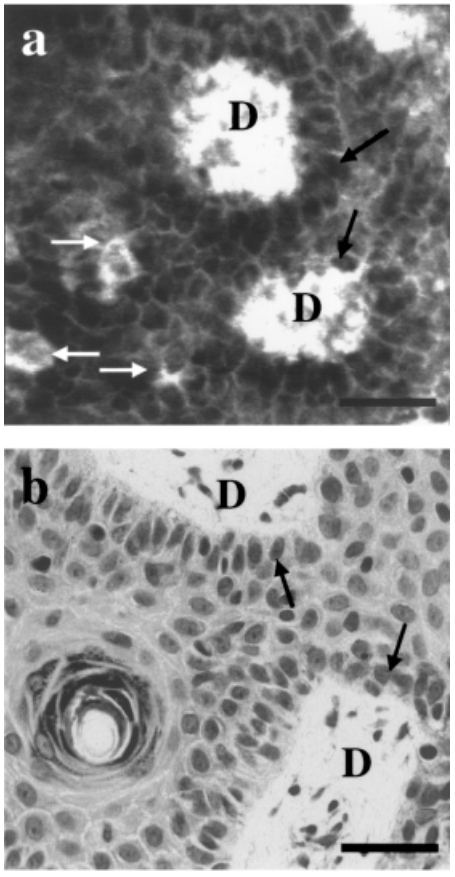

Figure 6. In the confocal image (*a*), dermal papillae (*D*) project into the overlying epidermis and appear as bright, regular, round, or elliptical structures. The lower left region shows the tips of dermal papillae (*white arrows*). A single layer of darker basal cells (*black arrows*) is arranged circumferentially around each papillae, as also seen in the comparative horizontal histology section (*b*). *Bar,* 25 μm.

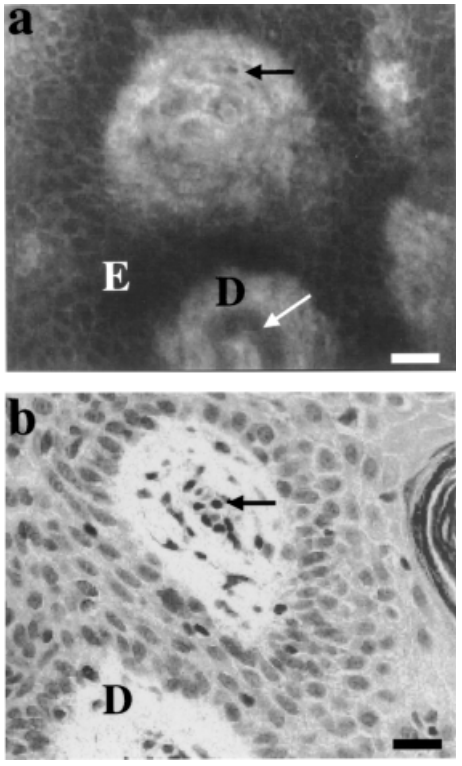

Figure 7. A capillary lumen (*white arrow*) is clearly visible in the dermal papillae (*D*) in the confocal image (*a*). Dark blood cells (*black arrows*) contrast with bright plasma in the lumen; so dynamic blood flow can be visualized in real-time imaging. The horizontal histology section gives a corresponding static view of capillaries (*b*). *Bar,* 25 μm.

fluorophore acting as a contrast agent. The results have demonstrated the epidermal cell layers with subcellular detail and we have observed dynamic processes occurring within the superficial layers of the dermis.

The imaging patterns observed using a fluorescent contrast agent were consistent and reproducible among the study sample. The morphologic patterns associated with major cell types of the epidermis were recognizable and consistent with histologic skin sections viewed by conventional microscopy. Certain other features were not identified with confidence and will require future detailed correlative studies with histology. Of particular note in the deeper regions of viable epidermis was the frequent presence of strongly fluorescent, variable-sized spots (3–5 μm) (**Fig 1*g***). These were initially suspected to be nuclei; however, their variation in size and inconsistency in distribution did not support this. It is postulated that these spots are extracellular fluorescein that has pooled owing to difficulty trafficking through desmosomal adhesions between cells. Alternatively, they may be the result of phagocytosis of the contrast agent into intracellular compartments by keratinocytes.

Many of the cells at the basal layer (which were seen surrounding the dermal papillae hilltops) had significantly darker cytoplasm compared to keratinocytes in the other layers (**Fig 6*a***). The appearance and location of these cells is consistent with that of melanocytes or heavily melanized basal keratinocytes sitting at the expected location immediately above the dermoepidermal junction. This observation of darker cytoplasm at the basal level was enhanced in individuals with darker pigmentation (skin types III and IV) compared to lightly pigmented skin (types I and II).

While the keratinocytes comprising the majority of the epidermal cell matrix could be identified with confidence, conclusive identification of particular cell types (e.g., melanocytes and Langerhans cells) and associated subcellular structures will need to be validated with further detailed morphologic examination and the use of immunologically targeted cell markers.

With *in vivo* confocal microscopy, subsurface imaging of tissue layers is achieved by noninvasive optical sectioning. The view of the tissue is parallel to the surface of the skin, which is orthogonal to the typical vertical orientation used in conventional histology (**Fig 2**). This *en face* view of skin requires new techniques of analysis, interpretation, and description that should ultimately complement and expand on the information gained by conventional techniques and other skin imaging modalities.

In vivo reflectance confocal imaging already has substantial momentum in the pursuit of the new paradigm of noninvasive skin imaging. This technique has been used to investigate inflammatory, keratinocytic, and pigmented skin lesions. Reflectance microscopy, as described in the majority of literature reports to date, exploits the distribution of naturally occurring refractive index variations and chemicals within skin to provide a source of contrast. For example melanin provides contrast when illuminated with light in the infrared spectrum (Rajadhyaksha *et al*, 1995). In the absence of exogenous reflective contrast agents, there is a limited potential to extract additional information from the tissue. Recent studies have been directed toward finding suitable contrast agents for reflectance imaging that may overcome this limitation (Rajadhyaksha *et al*, 2001; Zuluaga *et al*, 2002). The technique described in this study involves the use of an exogenous fluorescent contrast agent, and like the multitude of stains

used in conventional histology, different fluorescent contrast agents and protocols would have the ability to highlight different structures. This could greatly expand the range of applications and usefulness of *in vivo* fluorescence CSLM.

The pharmacokinetic processes that occur in living tissue such as metabolism by enzymes and clearance via vascular and lymphatic channels, or the permeability characteristics of individual cells will affect the distribution of contrast agent, and would therefore need to be taken into account in the interpretation of imaging patterns. These same processes also offer the potential to observe numerous dynamic functional aspects of living skin *in vivo*, through the selection of appropriate contrast agents and protocols. The use of intradermally administered fluorescein in this study represents just one of myriad possible protocols and "staining patterns."

For example, an area of much potential for fluorescence confocal microscopy lies in the ability to target specific subcellular molecules (including proteins) and therefore to monitor specific pathologic and immune processes over time. Preliminary studies using targeted fluorescent probes in animal models of melanoma have demonstrated that pathologic protein overexpression can be microscopically observed *in vivo* (Anikijenko *et al*, 2001).

The use of an exogenous contrast agent, however, also presents complexities in the interpretation of image contrast and may also impact the state of the tissue itself (Cullander, 1999; Rajadhyaksha and Gonzalez, 2003). Local physiologic factors such as clearance and redistribution, pH, and chemical quenching will all impact the pattern of fluorescence observed (Rajadhyaksha and Gonzalez, 2003; Sjoback *et al*, 1995; Song *et al*, 1995). Interestingly, such factors also make this imaging method a form of functional imaging, in which such interactions may be useful in the study of physiologic factors that influence them. Phototoxic effects causing potential negative alterations in the *in vivo* cellular environment are also a factor for consideration in fluorescence confocal microscopy (Saetzler *et al*, 1997; Zhang *et al*, 1997). In this study, no observations of photo bleaching were made, and no adverse events were reported in relation to the administration of sodium fluorescein or confocal microscopy. The particular conditions employed in our study relating to use of a clinically well-established fluorophore, low energy of illumination (by comparison to conventional usage of fluorescein), limited lens numerical aperture and relatively fast, and transient scanning on any particular microscopic field of view minimized the impact of such factors on our results.

Imaging depth is one of the key technical limitations that will define the scope of clinical applications for which the technology will be useful. The limit in depth is associated with the wavelength of laser light used. The 488-nm argon ion laser used in this study only allowed penetration and detection at the level of superficial papillary dermis and occasionally superficial reticular dermis. Optical coherence tomography, high-frequency ultrasound, and magnetic resonance imaging have superior depth penetration compared to *in vivo* confocal microscopy, but do not offer the resolution that enables the cellular detail of confocal microscopy (Tadrous, 2000). If confocal microscopy is to be useful in the study of pathologic processes that occur in the reticular dermis, these limitations will have to be overcome (for example, through the use of near-infrared laser sources in combination with exogenous fluorophores excited by such wavelengths).

The single-frame images captured and shown in our results are only representative of some of the information available via fluorescent confocal imaging. Imaging in real-time with operator interaction is preferable, providing a better appreciation of the relationships between structures observed in a continuum of images and spanning the undulating microarchitecture of the skin. It also allows real-time viewing of dynamic processes such as erythrocyte movement through capillaries. Development of tools for enhanced image review (e.g., capture and review of video streams) may facilitate further applications of this technology, which are enabled by this real-time aspect.

Fiber-optic fluorescence CSLM is currently an investigational imaging tool. CSLM is a widely accepted technique in the research field with major advancements in technology in recent years. Further investigations are needed, however, to ascertain a future role in the field of clinical dermatology. These initial results are compelling in their demonstration of real-time, microscopic views of living human skin *in vivo*, using a flexible handheld scanner. It will be a valuable tool in the study of diseases of the epidermis and dermoepidermal junction, whereas its capacity to target specific fluorescent molecules lends itself to application within the domains of skin-related pharmacology, immunology, and molecular biology. The challenge in developing this emerging imaging technique lies in the establishment of standard lexicons for image collection and interpretation, so that the new information may be integrated with that from existing accepted techniques, such as dermoscopy and histology. With this in mind, the expanding field of noninvasive skin imaging will continue to gain momentum. Preliminary *in vivo* and *ex vivo* studies using fluorescent contrast agents to investigate cell morphology within a variety of benign and malignant skin lesions suggest that there are observable and noteworthy differences in labeling patterns between normal skin and pathologic skin (Swindle *et al*, 2002). These early observations require further investigation and validation.

We thank Milind Rajadhyaksha for his assistance with the preparation of images for the manuscript. We thank Christina Lohmann and Klaus Busam from the pathology department at Memorial Sloan-Kettering Cancer Center for their assistance with the preparation and interpretation of histology sections.

REFERENCES

Aghassi D, Anderson RR, Gonzalez S: Confocal laser microscopic imaging of actinic keratoses in vivo: A preliminary report. *J Am Acad Dermatol* 43:42–48, 2000a

Aghassi D, Anderson RR, Gonzalez S: Time-sequence histologic imaging of laser-treated cherry angiomas with in vivo confocal microscopy. *J Am Acad Dermatol* 43:37–41, 2000b

Anikijenko P, Vo LT, Murr ER, *et al*: In vivo detection of small subsurface melanomas in athymic mice using noninvasive fiber optic confocal imaging. *J Invest Dermatol* 117:1442–1448, 2001

Bloom W, Fawcett DW: *A Textbook of Histology*, 10th ed. Philadelphia: Saunders, 1975: 10

Busam KJ, Charles C, Lee G, Halpern AC: Morphologic features of melanocytes, pigmented keratinocytes, and melanophages by in vivo confocal scanning laser microscopy. *Mod Pathol* 14:862–868, 2001a

Busam KJ, Hester K, Charles C, Sachs DL, Antonescu CR, Gonzalez S, Halpern AC: Detection of clinically amelanotic malignant melanoma and assessment of its margins by in vivo confocal scanning laser microscopy. *Arch Dermatol* 137: 923–929, 2001b

Bussau LJ, Vo LT, Delaney PM, Papworth GD, Barkla DH, King RG: Fibre optic confocal imaging (FOCI) of keratinocytes, blood vessels and nerves in hairless mouse skin in vivo. *J Anat* 192:187–194, 1998

Charles CA, Marghoob AA, Busam KJ, Clark-Loeser L, Halpern AC: Melanoma or pigmented basal cell carcinoma. A clinical-pathologic correlation with dermoscopy, in vivo confocal scanning laser microscopy, and routine histology. *Skin Res Technol* 8:282–287, 2002

Corcuff P, Chaussepied C, Madry G, Hadjur C: Skin optics revisited by in vivo confocal microscopy, melanin and sun exposure. *J Cosmet Sci* 52:91–102, 2001

Cullander C: Fluorescent probes for confocal microscopy. *Methods Mol Biol* 122:59–73, 1999

Delaney PM, Harris MR: Fibreoptics in confocal microscopy. In: Pawley EJ, (eds). *Handbook of Biological Confocal Microscopy*. New York: Plenum, 1995

Delaney PM, Harris MR, King RG: A fibre optic laser scanning confocal microscope suitable for fluorescence imaging. *Appl Opt* 33:573–577, 1994a

Delaney PM, Harris MR, King RG: Novel microscopy using fibre optic confocal imaging and its suitability for subsurface blood vessel imaging *in vivo*. *Clin Exp Pharmacol Physiol* 20:197–198, 1993

Delaney PM, King RG, Lambert JR, Harris MR: Fibre optic confocal imaging (FOCI) for subsurface microscopy of the colon *in vivo*. *J Anat* 184:157–160, 1994b

Gmitro A, Aziz D: Confocal microscopy through a fiber-optic imaging bundle. *Opt Lett* 18:565–567, 1993

Gonzalez S, Gonzalez E, White WM, Rajadhyaksha M, Anderson RR: Allergic contact dermatitis: Correlation of in vivo confocal imaging to routine histology. *J Am Acad Dermatol* 40:708–713, 1999a

Gonzalez S, Rajadhyaksha M, Gonzalez-Serva A, White WM, Anderson RR: Confocal reflectance imaging of folliculitis in vivo: Correlation with routine histology. *J Cutan Pathol* 26:201–205, 1999b

Gonzalez S, Rajadhyaksha M, Rubinstein G, Anderson RR: Characterization of psoriasis *in vivo* by reflectance confocal microscopy. *J Med* 30:337–356, 1999c

Gonzalez S, Tannous Z: Real-time, in vivo confocal reflectance microscopy of basal cell carcinoma. *J Am Acad Dermatol* 47:869–874, 2002

Juskaitis T, Wilson T, Watson TF: Real-time white light reflection confocal microscopy using a fibre-optic bundle. *Scanning* 19:15–19, 1997

Langley RG, Rajadhyaksha M, Dwyer PJ, Sober AJ, Flotte TJ, Anderson RR: Confocal scanning laser microscopy of benign and malignant melanocytic skin lesions *in vivo*. *J Am Acad Dermatol* 45:365–376, 2001

Liang C, Sung KB, Richards-Kortum RR, Descour MR: Design of a high-numerical-aperture miniature microscope objective for an endoscopic fiber confocal reflectance microscope. *Appl Opt* 41:4603–4610, 2002

New K, Petroll W, Boyde A, *et al*: *In vivo* imaging of human teeth and skin using real-time confocal microscopy. *Scanning* 13:369–372, 1991

Papworth GD, Delaney PM, Bussau LJ, Vo LT, King RG: *In vivo* fibre optic confocal imaging of microvasculature and nerves in the rat vas deferens and colon. *J Anat* 192:489–495, 1998

Rajadhyaksha M, Gonzalez S: Real-time *in vivo* confocal fluorescence microscopy. In: Myeck MA, Pogue B, (eds). *Handbook of Biomedical Fluorescence*. New York: Dekker, 2003: p. 143–179

Rajadhyaksha M, Gonzalez S, Zavislan JM, Anderson RR, Webb RH: *In vivo* confocal scanning laser microscopy of human skin. II. Advances in instrumentation and comparison with histology. *J Invest Dermatol* 113:293–303, 1999

Rajadhyaksha M, Grossman M, Esterowitz D, Webb RH, Anderson RR: *In vivo* confocal scanning laser microscopy of human skin: Melanin provides strong contrast. *J Invest Dermatol* 104:946–952, 1995

Rajadhyaksha M, Menaker G, Flotte T, Dwyer PJ, Gonzalez S: Confocal examination of non melanoma cancers in thick skin excisions to potentially guide Mohs micrographic surgery without frozen histopathology. *J Invest Dermatol* 117:1137–1143, 2001

Saetzler RK, Jallo J, Lehr HA, Philips CM, Vasthare U, Arfors KE, Tuma RF: Intravital fluorescence microscopy; Impact of light-induced phototoxicity on adhesion of fluorescently labeled leukocytes. *J Histochem Cytochem* 45:505–513, 1997

Sauermann K, Gambichler T, Wilmert M, Rotterdam S, Stucker M, Altmeyer P, Hoffmann K: Investigation of basal cell carcinoma by confocal laser scanning microscopy *in vivo*. *Skin Res Technol* 8:141–147, 2002

Sjoback R, Nygren J, Kubista M: Absorbtion and fluorescence properties of fluorescein. *Spectrochim Acta A* 51:7, 1995

Song L, Hennink EJ, Young IT, Tanke HJ: Photobleaching kinetics of fluorescein in quantitative fluorescence microscopy. *Biophys J* 68:2588–2600, 1995

Swindle LD, Delaney PM, Freeman M, *et al*: View of human skin *in vivo* as observed using fluorescence confocal microscopic imaging [abstract]. *Ann Dermatol Venereol* 129:1S602, 2002

Tadrous PJ: Methods for imaging the structure and function of living tissues and cells. 3. Confocal microscopy and micro-radiology. *J Pathol* 191:345–354, 2000

Thorn Leeson D, Lynn Meyers C, Subramanyan K: *In vivo* confocal fluorescence imaging of skin surface cellular morphology [abstract]. *OSA Biomedical Topical Meetings Technical Digest*, Optical Society of America: Washington DC: 2002: PD8-1

Veiro JA, Cummins PG: Imaging of skin epidermis from various origins using confocal laser scanning microscopy. *Dermatology* 189:16–22, 1994

Vo LT, Papworth GD, Delaney PM, Barkla DH, King RG: *In vivo* mapping of the vascular changes in skin burns of anaesthetised mice by fibre optic confocal imaging (FOCI). *J Dermatol Sci* 23:46–52, 2000

Zhang JL, Yokoyama S, Ohhashi T: Inhibitory effects of fluorescein isothiocyanate photoactivation on lymphatic pump activity. *Microvasc Res* 54:99–107, 1997

Zuluaga AF, Drezek R, Collier T, Lotan R, Follen M, Richards-Kortum R: Contrast agents for confocal microscopy: How simple chemicals affect confocal images of normal and cancer cells in suspension. *J Biomed Opt* 7:398–403, 2002